

Alma Mater Studiorum Università di Bologna
Archivio istituzionale della ricerca

Experimental Demonstration of MASH Based Sigma Delta Radio over Fiber System for 5G C-RAN Downlink

This is the final peer-reviewed author's accepted manuscript (postprint) of the following publication:

Published Version:

Hadi, M.U., Hadi, M.U., Aslam, N., Ali, R., Khurshid, K., Traverso, P.A., et al. (2022). Experimental Demonstration of MASH Based Sigma Delta Radio over Fiber System for 5G C-RAN Downlink. JOURNAL OF OPTICAL COMMUNICATIONS, 43(3), 457-463 [10.1515/joc-2019-0011].

Availability:

This version is available at: <https://hdl.handle.net/11585/696775> since: 2022-11-16

Published:

DOI: <http://doi.org/10.1515/joc-2019-0011>

Terms of use:

Some rights reserved. The terms and conditions for the reuse of this version of the manuscript are specified in the publishing policy. For all terms of use and more information see the publisher's website.

This item was downloaded from IRIS Università di Bologna (<https://cris.unibo.it/>).
When citing, please refer to the published version.

(Article begins on next page)

Muhammad Usman Hadi*, Muhammad Umair Hadi, Nelofar Aslam, Rafaqat Ali, Kiran Khurshid, Pier Andrea Traverso and Giovanni Tartarini

Experimental Demonstration of MASH based Sigma Delta Radio over Fiber System for 5G C-RAN Downlink

Abstract: Sigma Delta Radio over Fiber (S-DRoF) systems are looked upon as an enabling technology due to their advantages that comes due to combination of analog and digital radio over fiber systems. In this paper, we have proposed and experimentally demonstrated a Multi-stage-noise-SHaping (MASH) based Sigma Delta Modulated Radio over fiber system targeting 5G C-RAN (cloud/centralized radio access network) fronthaul applications. The evaluation has been done for LTE 20 MHz signal having 256 quadrature amplitude modulation with a carrier frequency of 3.5 GHz up to 5 Km of Standard Single Mode Fiber. Furthermore, a comprehensive analysis of the design is explained followed by the experimental setup. The performance is reported in terms of error vector magnitude and adjacent channel leakage ratio. It is concluded that S-DRoF substantiates the desired range of the 5G C-RAN fronthaul networks.

Keywords: Radio over Fiber, Sigma Delta Modulation, EVM, ACLR.

1 Introduction

In recent years, the continuous demand for delivering gigabits of data rate has become crucial. Next-generation networks such as 5G require high speed data rate, cost effective and low latency solutions [1]. In order to support such networks, a worthwhile and greener optical transport solution will be needed. Radio over Fiber (RoF) systems have been looked upon as a capacitive technology to cope with the on growing demand of these next generation networks. They can serve as a backbone for building the key enabler architecture solution known as centralized radio access network (C-RAN). Exploiting C-RAN, the optical distribution network known as ‘fronthaul’ is shown in Figure 1 [2]. Due to its inherent capillary properties, RoF technology is the most viable candidate for the 5G fronthauling [1-2]. The 5G C-RAN comprises of centralizing the Base Band Unit (BBU) of several base stations while keeping the relative Remote Radio Heads (RRHs) at the cell site.

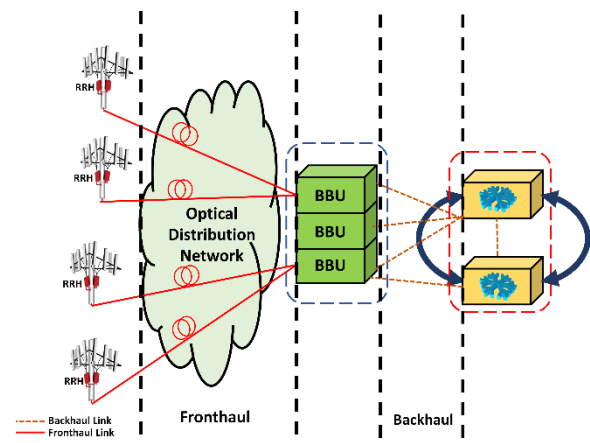


Figure 1: Basic C-RAN architecture

The techniques adapted for RoF can be either in analog or digital form. A-RoF offers the simplest solution in terms of complexity, however, nonlinearities coming from optical and microwave parts affect them adversely [3-5]. These nonlinearities can be compensated by utilizing Digital Predistortion [6-9] but these techniques are limited to narrow bandwidth and require feedback which is a difficult process.

Digital RoF (D-RoF) can overcome the nonlinear effects arising in A-RoF [10-11]. It has been regarded as a robust solution in terms of performance. However, the cost of D-RoF increases as the requirement of high precision analog to digital and digital to analog converters adds up to it. Similarly, the phase relation between many RRHs doesn't remain steady and spectral efficiency decreases [12]. Therefore, the existence of an alternative solution which can fix these bottlenecks would be desirable.

An auxiliary methodology is Sigma Delta Modulated Radio over Fiber (S-DRoF) that amalgamates the advantages of ARoF and DRoF [13-17]. This is a power efficient and robust technique eliminating the need for high-speed digital circuitry. The need of power hungry and high speed digital to analog converter (DAC) required in D-RoF is replaced by a sigma delta modulator ($\Sigma\Delta M$). The same RRH can be used for ARoF and S-DRoF. However, similar to D-RoF, the digital signal transmitted over the link is highly resistant to nonlinearities.

*Corresponding author: M.U. Hadi, Department of Electronic and Information Engineering, Viale Del Risorgimento 2, 40136, University of Bologna, Italy.

E-mail: muhammadusman.hadi2@unibo.it; usmanhadi@ieec.org

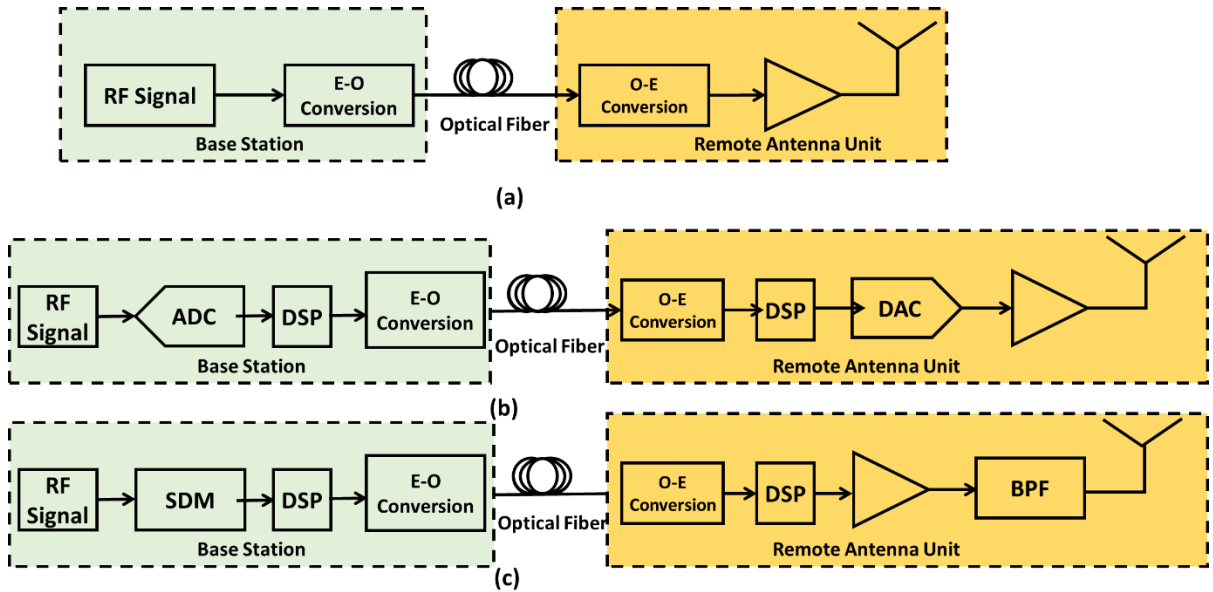


Figure 2: Schematic illustration of (a) A-RoF, (b) D-RoF and (c) S-DRoF. ADC: Analog to Digital Converter; DSP: Digital Signal Processor; E-O: Electrical-to-Optical; SMF: Single Model Fiber; O-E: Optical-to-Electrical; DAC: Digital to Analog Converter; SDM: Sigma Delta Modulation; BPF: Band Pass Filtering

In this paper, a novel and robust solution for the implementation of 5G CRAN downlink applications is proposed. The proposed system is based on Multi-stAge-noise-SHaping (MASH) Sigma-Delta (SD) modulator at the transmitter side, working as a 1-bit analog to digital converter (ADC). The Sigma delta modulation (SDM) is implemented in MATLAB. The paper is organized as follows. Section 2 summarizes the RoF architectures. Section 3 briefly discusses the Sigma Delta Radio over Fiber (S-DRoF) that employs the SDM to RF signal. Section 4 describes the system description. In Section 5, performance analysis of S-DRoF is presented in terms of Error Vector Magnitude (EVM) and Signal to Noise Ratio (SNR) while Section 6 concludes the paper

2 Radio over Fiber Architectures

In this section, the RoF architectures are summarized briefly. In Figure 2(a), the typical schematic of A-RoF is shown at the down link. The baseband signal is upconverted to RF signal which is then converted to an optical signal in electrical to optical (E-O) conversion block and transmitted through the optical link. At the receiver, optical to electrical (O-E) block retrieves the received RF signal back to electrical domain. This signal is then transmitted through the antenna after performing filtering and amplification.

Figure 2(b) represents the D-RoF schematic for the down-stream link. In the digitized RoF link, the analog RF signal is first converted to a digital signal through ADC and is transmitted over the optical fiber. The optical signal is photo detected at the receiver side and is converted back to analog domain using DAC. If required, this signal is upconverted to recover the original analog RF signal.

Figure 2(c) shows the S-DRoF schematic for the down link. In S-DRoF, a $\Sigma \Delta M$ is utilized to oversample the baseband signal followed by the quantization operation to one single bit. A digital up-converter moves the signal to the required center frequency. The band-pass filter (BPF) at the receiver end eliminates the out-of-band quantization noise carved by the SDM and insures that the channel mask requirements are met.

3 Multi-stAge-noise-SHaping (MASH) based $\Sigma \Delta M$

The objective of SDM operation is to eliminate the need of high speed and resolution ADC and DACs rather utilize low resolution stream of data at a sampling rate much higher than the Nyquist criteria. Therefore, the relatively high quantization noise can be reshaped in frequency domain so that the noise in the useful band can be reduced. This operation leads to a very high Signal to Noise Ratio (SNR) [18]. At the receiver end, the bandpass filtering (BPF) of the reshaped spectrum suppresses the quantization noise that results in retrieving of the original signal.

Figure 3 shows the schematic of the proposed $\Sigma \Delta M$ known as Multi stAge noise SHaping (MASH). It is designed using stages, where the next stage input is the quantization error introduced by the quantizer of the current stage, which is the difference between its output and input. The individual outputs are digitally filtered and combined in a way that the quantization noise of each stage, excluding the last, is canceled at the overall output of the structure.

A 2-stage MASH structure using a first order in each stage is shown in the Figure 3. In terms of signal transfer function (STF) and noise transfer function (NTF), the output of the first stage becomes:

$$y_1(z) = STF_1(z) * x(z) + NTF_1(z)Q_e(z) \quad (1)$$

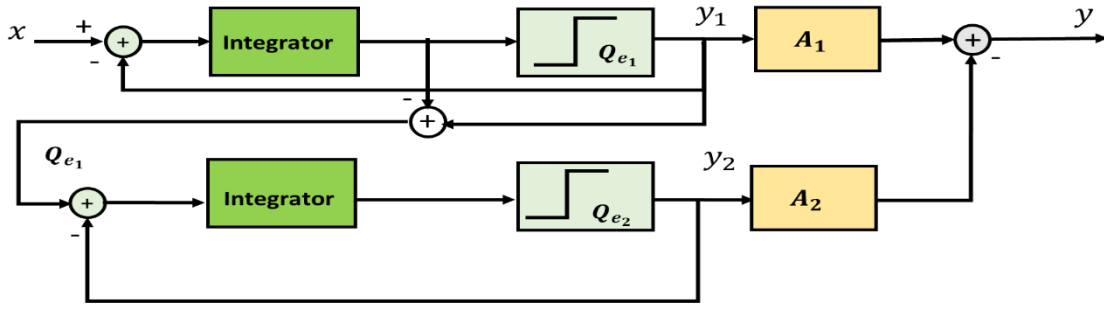


Figure 3: 2 Stage MASH $\Sigma \Delta M$ Structure

Similarly, the input of the second stage is the quantization error of the first stage. The output of second stage becomes:

$$y_2(z) = STF_1(z) * Q_{e1}(z) + NTF_1(z)Q_{e2}(z) \quad (2)$$

Moreover, the digital filters A_1 and A_2 must be designed at respective stages in order to cancel the quantization errors. The condition becomes:

$$A_1 \cdot NTF_1 + A_2 \cdot STF_2 == 0 \quad (3)$$

The overall output becomes:

$$\begin{aligned} y &= A_1 y_1 - A_2 y_2 \\ &= STF_1 \cdot STF_2 \cdot x - NTF_1 \cdot NTF_2 \cdot Q_{e2} \end{aligned} \quad (4)$$

By considering the first order $\Sigma \Delta M$ where $STF = z^{-1}$ and $NTF = 1 - z^{-1}$ as given in [19], we can write (4) as:

$$y(z) = z^{-2}x(z) - Q_{e2}(z)[1 - z^{-1}]^2 \quad (5)$$

From (5), the performance of a second order $\Sigma \Delta M$ is obtained. However, if second order $\Sigma \Delta M$ is used, the overall structure would have the noise shaping performance of a fourth order modulator. Stability of the structure is determined by the order of modulators used. Stability becomes a less important issue due to simplicity of the design stages since we utilize first order $\Sigma \Delta M$ in each stage of MASH.

Similarly, quantization error is employed as an input which is very close to true white noise reducing the need of dithering. Likewise, there is no harmonic distortion of the signal generated in these stages. Consequently, the MASH structure permits the use of multi-bit quantizer in the higher stages without requiring the need of correction of the DAC nonlinearity. The reason is that it is high-pass filtered by the NTF of the previous stage, suppressing it at the baseband.

4 System Description

The schematic of the experimental bench is shown in Figure 4. The RF signal is generated at digital signal processor (DSP) outvied by MATLAB. This RF signal is converted to 1-bit sigma delta modulation signal by MASH $\Sigma \Delta M$ implemented in MATLAB. The sigma delta modulated stream is then sent to Keysight 81134A Pulse Pattern Generator which directly modulates the Distributed Feedback (DFB) laser having 1550 nm wavelength. Single Mode Fiber (SMF) of length up to 5 Km is utilized in this experimental evaluation. The optical stream of transmitted data is converted into electrical domain by photodiode having 9.3 GHz of bandwidth. The photodiode output is fed to a low noise amplifier (LNA) followed by a BPF to filter the optical signal. This is followed by down conversion to baseband and further it is processed in evaluation block. The RF signal digitized by 1-bit MASH $\Sigma \Delta M$ is a 256 QAM modulated LTE signal of 20 MHz. The carrier frequency f_c is 3.5 GHz. The details of the parameters utilized are given in Table 1.

Table 1 - Systems Configuration

Parameter	Value
RF Signal	Carrier frequency = 3.5 GHz Constellation = 256QAM
Optical Link	Laser Wave Length= 1550 nm Average Power= 10 mW Line Width= 16e6 Hz
	Fiber Fiber Dispersion= 16 ps/nmkm Distance=0.1, 1, 2, 5 Km Attenuation= 0.5 $\frac{dB}{Km}$
	Photo-detector (PD) Responsivity 0.9 A/W Bandwidth: 9.3 GHz
Bandpass Filtering	Band Pass Bandwidth=190 MHz Conversion gain (Complete Receiver (PD+BPF))=220 V/W

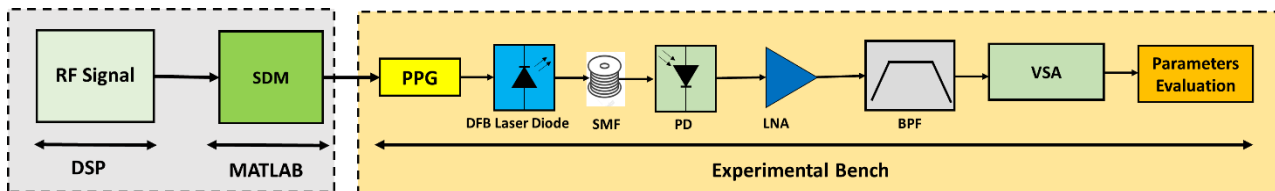


Figure 4: Experimental Bench for Sigma Delta Radio over Fiber system. SDM: Sigma Delta Modulation. SMF: Single Mode Fiber.

PPG: Pulse Pattern Generation. BPF: Band Pass Filtering. LNA: Low Noise Amplifier. VSA: Vector Signal Analyzer

5 Experimental Results and Discussion

In Sec. 5, the performances of the proposed S-DRoF are evaluated. At first, the performance of S-DRoF is firstly evaluated by the error vector magnitude (EVM). It is a quantity that assesses the difference between the “expected” complex value of a demodulated symbol w.r.t “actual” value of the received symbol. EVM can be mathematically expressed as [20]:

$$EVM (\%) = \sqrt{\frac{\frac{1}{M} \sum_{m=1}^M |S_m - S_{0,m}|^2}{\frac{1}{M} \sum_{m=1}^M |S_{0,m}|^2}} \quad (6)$$

where S_m is the normalized m^{th} symbol in the stream of measured symbols, M is the number of unique symbols in the constellation and $S_{0,m}$ is the ideal normalized constellation point of the m^{th} symbol. The 3GPP has set an EVM limit of 3.5% for LTE signals modulated by 256 QAM modulation format [21]. The performance is measured for various symbol rates up to 400 Mbd and for different fiber lengths up to 5 Km at 0 dBm of RF input power. The results are shown in Figure 6. The degradation in EVM performance is observed for all the fiber lengths. The reason for the degradation is that the received signal has low power due to the path loss.

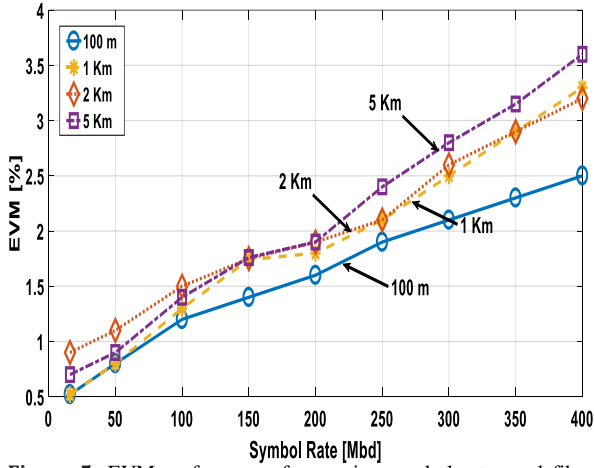


Figure 5: EVM performance for varying symbol rates and fiber lengths.

In Figure 6, the performance is expressed by varying the distance length up to 5 Km for varying input RF powers keeping in mind the fact that front haul lengths are generally in this order. It is observable that from -15 dBm of RF input power, EVM is in the limits for all the link lengths set by the 3GPP for 256 QAM.

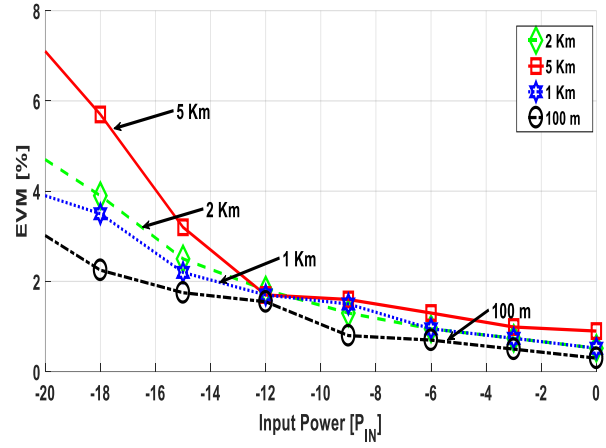


Figure 6: EVM performance for varying input powers and fiber lengths.

Now, the performance of the proposed S-DRoF is evaluated by measuring the adjacent leakage ratio (ACLR). It is defined as [7-8]:

$$ACLR (dB) = 10 \log_{10} \left[\frac{\int_{adjacent_band_l}^{adjacent_band_u} S(f) df}{\int_{useful_band_l}^{useful_band_u} S(f) df} \right] \quad (7)$$

where $useful_band_l$ and $useful_band_u$ are the upper and lower frequency limits of the useful channel respectively. $adjacent_band_l$ and $adjacent_band_u$ are the frequency limits of the adjacent channel while $S(f)$ is the Power Spectral Density (PSD) of the output signal. The ACLR is evaluated by changing the fiber length up to 5 Km. The RF input power is varied from -15 dBm to 0 dBm. The behavior is shown in Figure 7. Since higher input power leads to higher order of distortions in the adjacent channels, therefore ACLR rises.

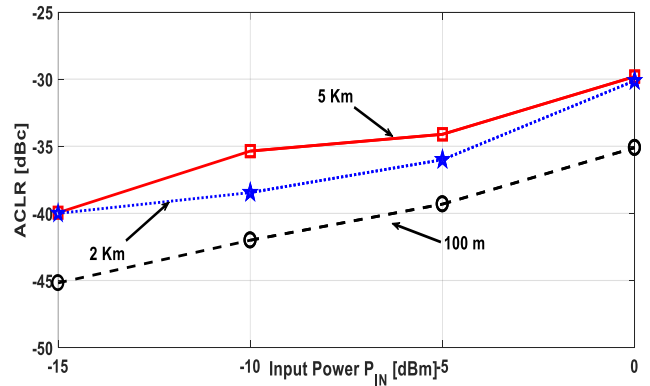


Figure 7: ACLR performance for varying RF input power and varying fiber lengths.

The transmission performance of the proposed S-DRoF is investigated by Eye diagrams of the transmitted signals. systems. The Eye-Opening Penalty (EOP) defines the deterioration in the eye diagrams. EOP is the ratio of the non-distorted reference eye called Eye Opening Amplitude (EOA) to the eye opening of the distorted eye, i.e. the Eye Opening Height (EOH) [22]. EOP is defined in (8) as:

$$EOP(dB) = 10 \log \left(\frac{EOA}{EOH} \right) \quad (8)$$

Figure 8 reports the EOP versus fiber length. It shows that the EOP increases with the increasing fiber length. In the S-DRoF case, the EOH does not closes. The inset at 5 Km also shows that the eye remains clean and wide open.

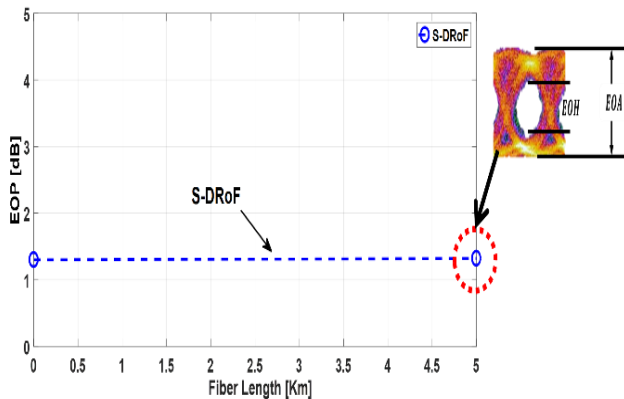


Figure 8: EOP versus Fiber length for 0 dBm of input power

The summary of the comparative overview of the parameters evaluated is given in Table II for the maximum and minimum length utilized for -5 dBm of input power at 400 Mbd.

Table II – Performance Summary at -5 dBm for 400 Mbd

Length (Km)	EVM (%)	ACPR (dBc)
0.1	2.5	-39.31
5	3.55	-34.11

Since this technique is meant to be utilized for 5G sub-6GHz band fronthaul applications, its cost analysis is important factor. Since SDM trades quantization bit for sampling rate, using high sampling rate and only few (1-bit generally) quantization bits, the need of very expensive and high-speed digital circuitry is not required. In case of CPRI, D-RoF systems at the remote antenna units (RAU) require a DAC which needs to be high speed and efficient enough to handle the operations. In case of S-DRoF, the deployment of DAC is replaced by a band pass filter which further decreases the cost. DSP kit is required for both, D-RoF and S-DRoF, so, the cost of DSP kit remains constant. However, one major challenge to both D-RoF and S-DRoF is the need of high processing speed. Sigma delta modulation requires high oversampling ratio to achieve the performance. To overcome the speed limit of existing FPGA, several parallel processing techniques have been reported, including polyphase decomposition [23,24] and look-ahead time-interleaving [25,26]. This means that by employing these techniques, even a simple FPGA kit can be deployed for the S-DRoF. This methodology greatly reduces the cost of S-DRoF to some thousands of euros as compared to D-RoF that will cost tens of thousands of euros for the same parameters and application. On basis of these facts, it can be proposed that S-DRoF is much cheaper solution than D-RoF systems.

6 Conclusions

In this paper, we have performed a novel demonstration experimentally for MASH based Sigma Delta Radio over Fiber for 5G sub-6GHz band fronthaul applications. By employing MASH, the second order SDM

performance can be obtained. Utilization of proposed system eliminates the need for high-speed ADCs and DACs required in D-RoF systems. The experimental workbench has been evaluated for LTE signal of 20 MHz bandwidth having 256 QAM modulation which is modulated on a 3.5 GHz carrier frequency at 1550 nm. The measurement results show that this methodology is suitable for transmitting LTE signals. The real time implementation of MASH based S-DRoF is achievable with FPGA which is currently under investigation and will be the target of a subsequent publication.

Acknowledgements

M.U.Hadi would like to extend his gratitude to the Nokia Bell Labs for fruitful discussion and collaboration.

References

1. A. Gupta and R. K. Jha, "A Survey of 5G Network: Architecture and Emerging Technologies," IEEE Access, Vol. 3, p. 1206- 1232 (2015)
2. China Mobile Research Institute, Beijing, China, "C-RAN: the Road Towards Green RAN," White Paper (2013).
3. C. Ranaweera, E. Wong, A. Nirmalathas, C. Jayasundara and C. Lim, "5G C-RAN with Optical Fronthaul: an Analysis from a Deployment Perspective," J. Lightw. Technol., Vol. 36, no. 11, p. 2059-2068 (2018).
4. T. Kurniawan, A. Nirmalathas, C. Lim, D. Novak, and R. Waterhouse, "Performance analysis of optimized millimeter-wave fiber radio links," IEEE Trans. Microwave Theory Tech. 54, 921–928 (2006).
5. Gagnaire M. (2017) Analog and Digitized Radio-over-Fiber. In: Tomatore M., Chang GK., Ellinas G. (eds) Fiber-Wireless Convergence in Next-Generation Communication Networks. Optical Networks. Springer, Cham
6. F. Fuochi, M. U. Hadi, J. Nanni, P. A. Traverso and G. Tartarini, "Digital predistortion technique for the compensation of nonlinear effects in radio over fiber links," 2016 IEEE 2nd International Forum on Research and Technologies for Society and Industry Leveraging a better tomorrow (RTSI), Bologna, 2016, pp. 1-6. doi:10.1109/RTSI.2016.7740562
7. M. U. Hadi, J. Nanni, P. A. Traverso, G. Tartarini, O. Venard, G. Baudoin and J. L. Polleux, "Experimental evaluation of digital predistortion for VCSEL-SSMF-based Radio-over-Fiber link. 2018, 2018 IEEE International Topical Meeting on Microwave Photonics (MWP), Vol. 1, pp. 1-4,
8. M. U. Hadi, P. A. Traverso, G. Tartarini, O. Venard, G. Baudoin and J. L. Polleux, "Digital Predistortion for Linearity Improvement of VCSEL-SSMF-based Radio-over-Fiber Links," in IEEE Microwave and Wireless Components Letters, Jan. 2019 (early access) DOI: 10.1109/LMWC.2018.2889004
9. A. Hekkala et al., "Predistortion of Radio Over Fiber Links: Algorithms, Implementation, and Measurements," in IEEE Transactions on Circuits and Systems I: Regular Papers, vol. 59, no. 3, pp. 664-672, March 2012.
10. P. A. Gamage, A. Nirmalathas, C. Lim, D. Novak, and R. Waterhouse, "Design and analysis of digitized RF-over-fiber links," IEEE J. Lightw. Technol., vol. 27, p. 2052–2061, June 2009.
11. Y. Yang, C. Lim, and A. Nirmalathas, "Experimental demonstration of multi-service hybrid fiber-radio system using digitized RF-over-fiber technique," IEEE J. Lightw. Technol., vol. 29, pp. 2131–2137, July 2011.
12. A. Haddad and M. Gagnaire, "Radio-over-Fiber (RoF) for mobile backhauling: A technical and economic comparison between analog and digitized RoF," in Proc. Int. Conf. Opt. Netw. Design Modeling, May 2014, pp. 132–137
13. L. Breyne, G. Torfs, X. Yin, P. Demeester and J. Bauwelinck, "Comparison between analog radio-over-fiber and sigma delta modulated radio-over-fiber," IEEE Photonics Technology, Vol. 29, 1808-1811, 2017
14. L. M. Pessoa, J. S. Tavares, D. Coelho, and H. M. Salgado, "Experimental evaluation of a digitized fiber-wireless system

- employing sigma delta modulation,” *Opt. Express*, vol. 22, no. 14, pp. 17508–17 523, Jul 2014.
15. S. Jang, G. Jo, J. Jung, B. Park, and S. Hong, “A digitized if-over fiber transmission based on low-pass delta-sigma modulation,” *IEEE Photonics Technology Letters*, vol. 26, no. 24, pp. 2484–2487, Dec 2014.
 16. Hadi, M., Aslam, N. & Jung, H. (2019). Performance Appraisal of Sigma Delta Modulated Radio over Fiber System . *Journal of Optical Communications*, 0(0), pp. -Jan. 2019, from doi:10.1515/joc-2018-0227
 17. D. Markert, X. Yu, H. Heimpel, and G. Fischer, “An all-digital, singlebit rf transmitter for massive mimo,” *IEEE Transactions on Circuits and Systems I: Regular Papers*, vol. 64, no. 3, pp. 696–704, March 2017
 18. R. Schreier and G. C. Temes, *Understanding Delta-Sigma Data Converters*, 1st ed. Hoboken, NJ, USA: Wiley, 2004.
 19. David Fouto, Nuno Paulino, *Design of Low Power and Low Area Passive Sigma Delta Modulators for Audio Applications*, springer, ISSN 2191-8112 ISSN 2191-8120 (electronic) SpringerBriefs in Electrical and Computer Engineering. ISBN 978-3-319-57032-7 ISBN 978-3-319-57033-4 (eBook) DOI 10.1007/978-3-319-57033-4
 20. Forestier, S.; Bouvsse, P., Quere, R., Mallet, A., Nebus, J.M., Lapiere, L.: Joint optimization of the power-aided efficiency and error vector measurement of 20-GHz pHEMT amplifier through a new dynamic bias-control method. *IEEE Trans. Microwave Theory Tech.* 52(4), 1132-1140 (2004)
 21. 3GPP TS36.101 V12.6.0, Evolved Universal Terrestrial Radio Access (E-UTRA) User Equipment (UE) Radio Transmission and Reception (Release 12), December 2014
 22. Seimetz, M.: ‘System Simulation Aspects’ in ‘HighOrder Modulation for Optical Fiber Transmission’, (Springer, 2009), pp. 127-131.
 23. R. F. Cordeiro, A. S. R. Oliveira, J. Vieira and T. O. e Silva, “Wideband all-digital transmitter based on multicore DSM,” *IEEE MTT-S International Microwave Symposium (IMS) 2016*.
 24. D. C. Dinis, R. F. Cordeiro, A. S. R. Oliveira, J. Vieira and T. O. Silva, “Improving the performance of all-digital transmitter based on parallel delta-sigma modulators through propagation of state registers,” *IEEE 60th International Midwest Symposium on Circuits and Systems (MWSCAS) 2017*, pp. 1133-1137.
 25. M. Tanio, S. Hori, N. Tawa, T. Yamase and K. Kunihiro, “An FPGA-based all-digital transmitter with 28-GHz time-interleaved delta-sigma modulation,” *IEEE MTT-S International Microwave Symposium (IMS) 2016*.
 26. M. Tanio, S. Hori, N. Tawa and K. Kunihiro, “An FPGA-based all-digital transmitter with 9.6-GHz 2nd order time-interleaved delta-sigma modulation for 500-MHz bandwidth,” *IEEE MTT-S International Microwave Symposium (IMS) 2017*, pp. 149-152